Applied Catalysis A: General 415–416 (2012) 141–148

Contents lists available at SciVerse ScienceDirect

Applied Catalysis A: General

journal homepage: www.elsevier.com/locate/apcata

Hydrogenation of succinic acid to tetrahydrofuran (THF) over rhenium catalyst supported on H_2SO_4-treated mesoporous carbon

Ung Gi Hong, Hai Woong Park, Joongwon Lee, Sunhwan Hwang, Jongheop Yi, In Kyu Song*

School of Chemical and Biological Engineering, Institute of Chemical Processes, Seoul National University, Shinlim-dong, Kwanak-ku, Seoul 151-744, South Korea

ARTICLE INFO

Article history:
Received 30 September 2011
Received in revised form 7 December 2011
Accepted 13 December 2011
Available online 21 December 2011

Keywords:
Hydrogenation
Succinic acid
Mesoporous carbon
Rhenium
Tetrahydrofuran

ABSTRACT

Mesoporous carbon (MC) prepared by a surfactant-templating method was treated with different H_2SO_4 concentration ($X = 0, 0.2, 0.4, 0.6, 0.8$, and 1.0 M) for use as a support (MC-X) for rhenium catalyst. Rhenium catalysts supported on H_2SO_4-treated mesoporous carbons (Re/MC-X) were then prepared by an incipient wetness impregnation method, and they were applied to the liquid-phase hydrogenation of succinic acid to tetrahydrofuran (THF). The effect of H_2SO_4 treatment on the physicochemical properties and catalytic activity of Re/MC-X catalysts ($X = 0, 0.2, 0.4, 0.6, 0.8$, and 1.0) was investigated. It was observed that MC-X supports showed different pore characteristics depending on H_2SO_4 concentration. As a result, Re/MC-X catalysts showed different rhenium particle size. In the liquid-phase hydrogenation of succinic acid to tetrahydrofuran (THF), conversion of succinic acid and yield for THF showed volcano-shaped curves with respect to H_2SO_4 concentration. Thus, an optimal H_2SO_4 concentration was required to achieve maximum catalytic performance of Re/MC-X. Yield for THF in the hydrogenation of succinic acid increased with decreasing rhenium particle size of Re/MC-X catalysts. Among the catalysts tested, Re/MC-0.4 with the smallest rhenium particle size showed the highest yield for THF.

1. Introduction

Tetrahydrofuran (THF) is widely used as a solvent in various industries. Polymerization of THF gives a raw material for manufacturing polytetramethylene ether glycol (PTMEG), thermoplastic polyesters, and polyurethane elastomers [1–3]. THF is currently produced via several routes including hydrogenation of maleic anhydride (MAN) [4], dehydration of 1,4-butanediol (BDO) [5], and oxidation of butadiene (BD) [6]. However, all these feedstocks (MAN, BDO, and BD) are obtained from fossil fuels, leading to unstable price and environmental problems. Therefore, demand for finding a cheap and green chemical that can replace these feedstocks has continuously increased [7–9]. Recently, conversion of succinic acid to THF has attracted much attention, because of the increase of succinic acid production in the biorefinery process [10,11]. Succinic acid is a cheap and bio-based chemical that can be converted into THF by hydrogenation reaction.

Hydrogenation of succinic acid (SA) to THF follows two consecutive reaction steps (Fig. 1). First, cyclization occurs by hydrogenation of carboxyl group in succinic acid to form γ-butyrolactone (GBL). Second, THF is formed via oxidative hydrogenation of carbonyl group in GBL. It is known that noble metal catalysts such as platinum, palladium, ruthenium, and rhenium are efficient in the hydrogenation of succinic acid to GBL [12,13]. For the production of THF, however, strong activity for hydrogenation of carbonyl group is also required. Therefore, it is important to find a suitable noble metal catalyst that has both cyclization activity (SA → GBL) and oxidative-hydrogenation activity (GBL → THF) in the hydrogenation of succinic acid to THF. It is known that rhenium catalyst causes complete reduction of both carboxyl and carbonyl groups, leading to further hydrogenation of GBL [14]. Therefore, rhenium catalyst can be a potential candidate for selective production of THF in the hydrogenation of succinic acid.

Noble metal catalysts have been generally used as supported catalysts to increase metal dispersion, because of high price of noble metal [15]. Therefore, it is also important to find efficient supporting materials. Among various supporting materials, ordered mesoporous carbon has found successful applications in many reactions due to its well-developed porosity, non-toxicity, and hydrophobic property [16–18]. In particular, regularly developed mesoporosity of carbon support is a very important property to increase metal dispersion in the supported noble metal catalyst system. If carbon support is prepared to have a controllable pore structure for increasing rhenium dispersion, therefore, it can serve as an excellent support for rhenium catalyst to obtain hydrogenation product of succinic acid with high catalytic activity.

It has been reported that surface area and pore volume of mesoporous carbon material prepared by a surfactant-templating

---

* Corresponding author. Tel.: +82 2 880 9227; fax: +82 2 889 7415.
E-mail address: inksong@snu.ac.kr (I.K. Song).

0926-860X/$ – see front matter © 2011 Elsevier B.V. All rights reserved.
doi:10.1016/j.apcata.2011.12.022

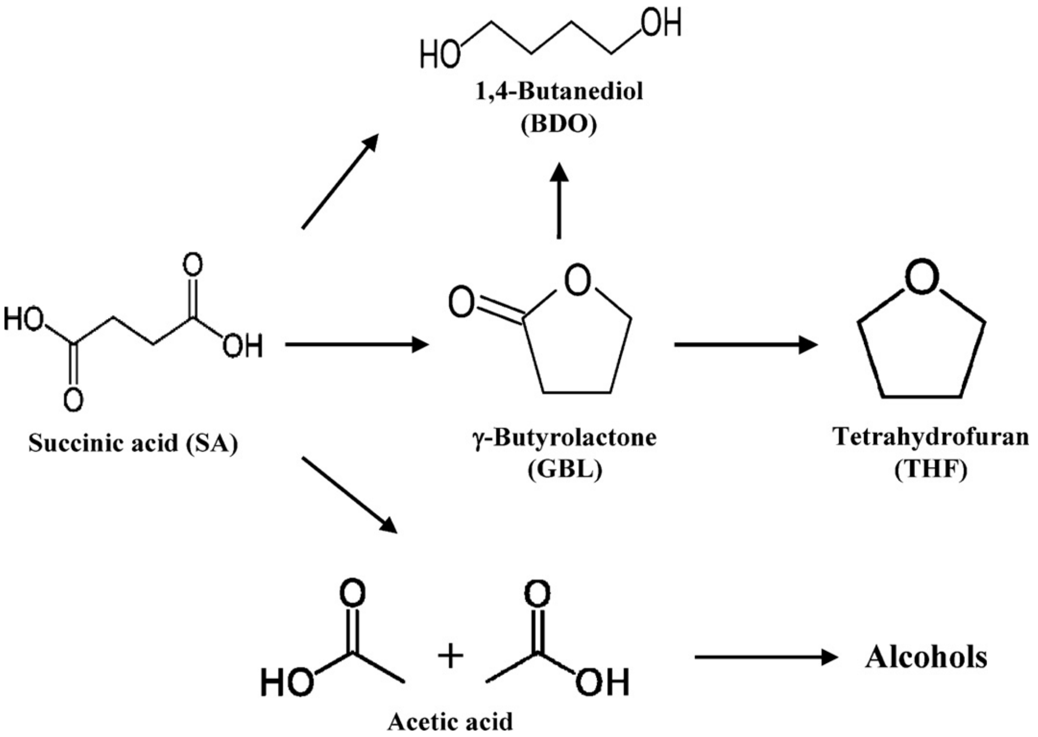

Fig. 1. Reaction pathways for the conversion of succinic acid.

method can be controlled by acid treatment [19,20]. Furthermore, mesoporous carbon prepared by a surfactant-templating method not only yields a highly ordered pore structure but also provides a simple preparation route. Therefore, it is expected that mesoporous carbon prepared by a surfactant-templating method can serve as an excellent supporting material if it is properly treated.

In this work, mesoporous carbon (MC) was prepared by a surfactant-templating method. MC was then treated with different H_2SO_4 concentration with an aim of controlling pore characteristics. Rhenium catalysts supported on H_2SO_4-treated MC were prepared by an incipient wetness impregnation method. The supports and supported catalysts were characterized by FE-SEM, HR-TEM, SAXS, N_2 adsorption–desorption isotherm, and TPR analyses. Liquid-phase hydrogenation of succinic acid to THF was carried out over the supported rhenium catalysts in a batch reactor. The effect of H_2SO_4 treatment on the physicochemical properties and catalytic activity of supported rhenium catalysts was investigated.

2. Experimental

2.1. Preparation of supported rhenium catalysts

Fig. 2 shows the schematic procedures for the preparation of mesoporous carbon (MC). A carbon precursor (sucrose, 8 g, Aldrich) and P123 (tri-block copolymer surfactant, 16 g, Aldrich) were dissolved in 4 M HCl solution (300 ml) at 40 °C for 4 h under stirring. After a silica precursor (TEOS, 36 ml, Aldrich) was slowly added into the solution, the resultant was dried overnight at 100 °C. The resulting precipitate was washed and filtered with de-ionized water, and it was then dried at 80 °C to obtain a sucrose/surfactant/silica composite. To control pore characteristics, 20 g of composite was treated with 400 ml of H_2SO_4 solution with different concentration (0, 0.2, 0.4, 0.6, 0.8, and 1.0 M) for 12 h. After drying the mixture at 160 °C for 8 h, the resulting brown solid was carbonized at 800 °C for 4 h at a heating rate of 5 °C/min in a nitrogen stream (100 ml/min). The resultant was further treated with 5 wt% HF solution to remove silica template. The resulting mesoporous carbon treated with different H_2SO_4 concentration (X = 0, 0.2, 0.4, 0.6, 0.8, and 1.0 M) was denoted as MC-X (MC-0, MC-0.2, MC-0.4, MC-0.6, MC-0.8, and MC-1.0), where X represented H_2SO_4 concentration.

For comparison, porous carbon (PC) and carbon aerogel (CA) supports were also prepared with H_2SO_4 treatment. For the preparation of porous carbon, a carbon precursor (sucrose, 8 g, Aldrich) was dissolved in 4 M HCl solution (300 ml) at 40 °C. After a silica precursor (TEOS, 36 ml, Aldrich) was slowly added into the solution, the resultant was dried at 100 °C. The resulting powder (20 g) was then treated with 0.4 M H_2SO_4 solution (400 ml) for 12 h. After drying the mixture at 160 °C for 8 h, the resulting solid was carbonized at 800 °C for 4 h at a heating rate of 5 °C/min in a nitrogen stream (100 ml/min). The resultant was further treated with 5 wt% HF solution to remove silica template. The porous carbon support treated with 0.4 M H_2SO_4 solution was denoted as PC-0.4.

For the preparation of carbon aerogel, RF (resorcinol–formaldehyde) sol–gel method was employed as reported in the literatures [21,22]. 25.9 g of resorcinol (Aldrich) was dissolved in 60.0 ml of DI water. Aqueous resorcinol was mixed with Na_2CO_3 (0.05 g) to accelerate dehydrogenation of resorcinol. After stirring the solution for a few minutes, 14.1 g of formaldehyde (Aldrich) was slowly added into the solution to form a sol. The resulting sol was heated to produce resorcinol–formaldehyde (RF) gel at 80 °C for 24 h. Acetone exchange was performed at 50 °C for two days. Residual solvent was replaced with fresh acetone every 3 h to remove water thoroughly from the pore of RF wet gel. Ambient drying was then done at room temperature for one day. The resulting solid (20 g) was then treated with 0.4 M H_2SO_4 solution (400 ml) for 12 h. After drying the mixture at 160 °C for 8 h, the solid was carbonized at 800 °C for 4 h at a heating rate of 5 °C/min in a nitrogen stream (100 ml/min). The carbon aerogel support treated with 0.4 M H_2SO_4 solution was denoted as CA-0.4.

Rhenium catalysts supported on H_2SO_4-treated carbons (Re/MC-0, Re/MC-0.2, Re/MC-0.4, Re/MC-0.6, Re/MC-0.8, Re/MC-1.0, Re/CA-0.4, and Re/PC-0.4) were prepared by an incipient wetness impregnation method using an acetone solution of rhenium chloride precursor ($ReCl_5$, Aldrich). Rhenium loading was

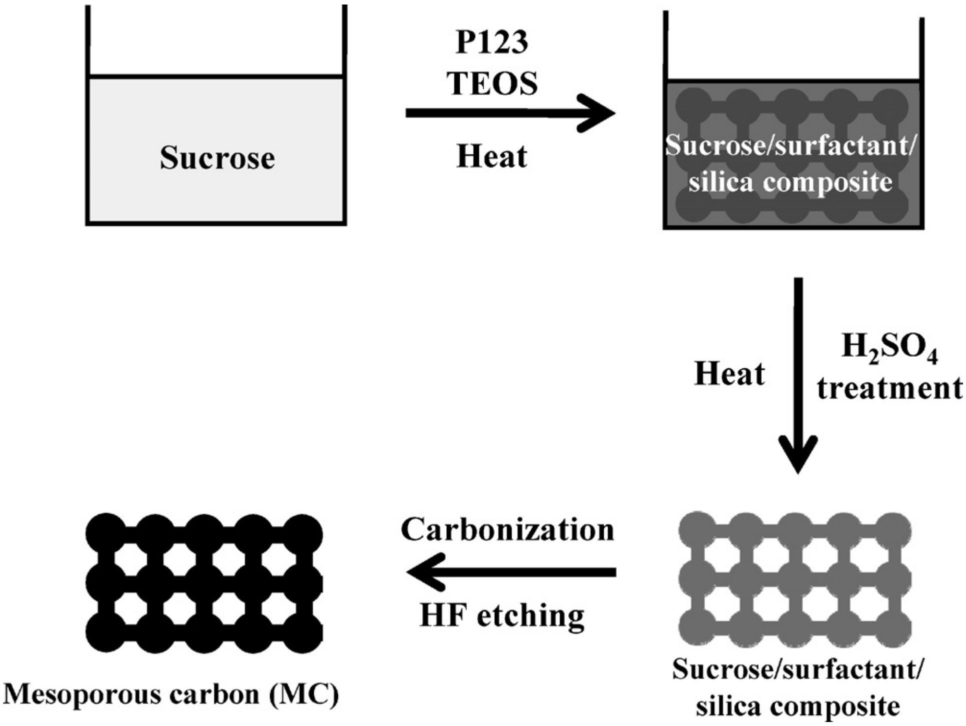

Fig. 2. Schematic procedures for the preparation of MC support.

fixed at 5 wt% in all the catalysts. After calcining the supported catalysts at 500 °C in a nitrogen stream, they were dried overnight at 80 °C. The dried catalysts were then reduced with a mixed stream of hydrogen (2.5 ml/min) and nitrogen (47.5 ml/min) at 450 °C prior to the catalytic reaction.

2.2. Characterization

Morphologies of carbon supports (MC-0, MC-0.2, MC-0.4, MC-0.6, MC-0.8, and MC-1.0) were examined by FE-SEM analyses (Jeol, JSM-6700F). Nitrogen adsorption–desorption isotherms of supported catalysts (Re/MC-0, Re/MC-0.4, and Re/MC-0.8) were obtained with an ASAP-2010 instrument (Micromeritics). Surface areas and pore volumes of supported catalysts were calculated using the BET equation and the BJH model, respectively. Crystalline state of carbon supports was examined by SAXS (small-angle X-ray scattering) measurements. SAXS patterns of MC-*X* supports were obtained with a Bruker GADDS instrument using $\lambda = 1.54$ Å radiation. Rhenium dispersion was examined by HR-TEM (Jeol, JEM-3000F) analyses. Hydrogen uptake and metal–support interaction of supported catalysts (Re/CA-0.4, Re/PC-0.4, and Re/MC-*X*) were examined by TPR (temperature programmed reduction) experiments using a conventional flow system equipped with a TCD (thermal conductivity detector) at temperatures ranging from 150 to 450 °C with a ramping rate of 5 °C/min. For TPR measurements, a mixed stream of H_2 (2 ml/min) and N_2 (20 ml/min) was used for 0.05 g of catalyst sample.

2.3. Hydrogenation of succinic acid

Liquid-phase hydrogenation of succinic acid (SA) to THF was carried out over supported rhenium catalysts in a batch reactor at 240 °C and 80 bar (H_2). Succinic acid (0.5 g) and a reduced catalyst (0.2 g) were charged into an autoclave (150 ml). 1,4-Dioxane (50 ml) was used as a solvent for the reaction. The reactor was purged with nitrogen to remove air, and then it was pressurized up to 40 bar using hydrogen. After heating the reactor to reaction temperature (240 °C), hydrogen pressure was raised up to 80 bar. The catalytic reaction was carried out for 8 h. During the reaction, reaction mixture was stirred at 500 rpm in order to avoid mass transfer limitation. Reaction products were analyzed using a gas chromatograph (Younglin, ACME-6100) equipped with a FID (flame ionization detector). In order to investigate the stability of the catalyst, the amount of rhenium leaching was measured by ICP-AES (PerkinElmer, Optima-4300DV) measurements.

3. Results and discussion

3.1. Morphology and crystalline structure of MC-X supports

Fig. 3 shows the FE-SEM images of MC-*X* ($X = 0$, 0.2, 0.4, 0.6, 0.8, and 1.0) supports. Pore structure and surface morphology of MC-*X* ($X = 0$, 0.2, and 0.4) supports showed fairly regular arrangement with increasing H_2SO_4 concentration. On the other hand, pore structure of MC-*X* ($X = 0.6$, 0.8, and 1.0) supports was collapsed with increasing H_2SO_4 concentration. These results indicate that there is an optimal H_2SO_4 concentration for obtaining well-developed pore structure. It is reported that polymeric chains of surfactant (P123) can be converted into carbon materials by dehydration and calcination [19,20]. H_2SO_4 may act as a catalyst to dehydrate hydroxyl group of cross-linked polymer chain of P123. These cross-linked polymer chains are converted into carbon materials during the calcination step. This means that surfactant performs the role of template framework as well as the role of carbon source together with sucrose. However, H_2SO_4 treatment at high concentration may cause destruction of pore channel. Therefore, an optimal H_2SO_4 concentration was required to obtain ordered mesoporosity in the surfactant-templating method. Among the MC-*X* supports, MC-0.4 support showed the most regular pore structure and surface morphology.

In order to investigate accurate crystalline structure of MC-*X* ($X = 0$, 0.2, 0.4, 0.6, 0.8, and 1.0) supports, SAXS analyses were performed. Fig. 4 shows the SAXS patterns of MC-*X* supports. The (1 0 0), (1 1 0), and (2 0 0) reflections appeared in MC-0.2, MC-0.4,

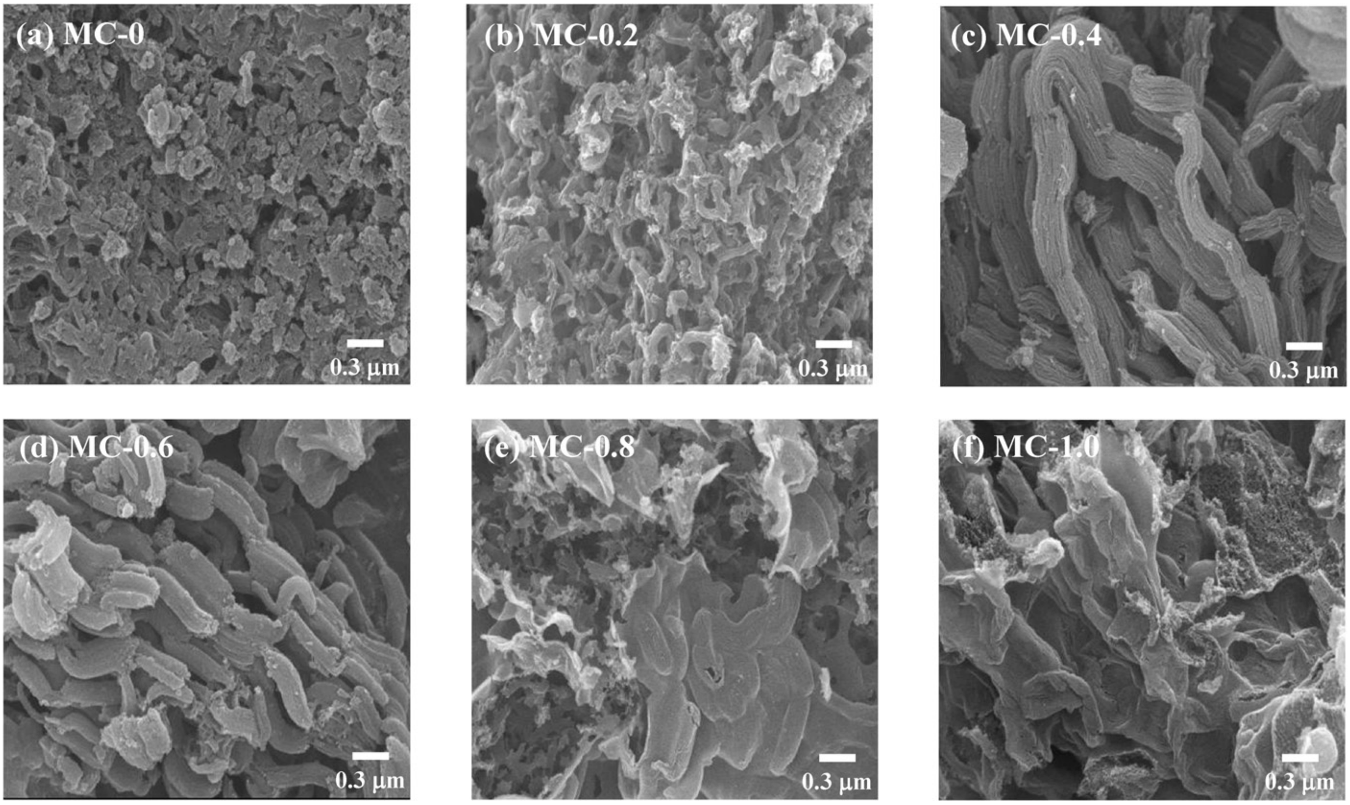

Fig. 3. FE-SEM images of MC-*X* supports.

and MC-0.6 samples. In particular, MC-0.4 showed the most obvious scattering peaks. These three characteristic peaks correspond to diffraction of 2-D hexagonal space group (*p6mm*), demonstrating long-range ordering of carbon material [23,24]. This implies that MC-0.4 support has the most regular pore structure among the MC-*X* supports.

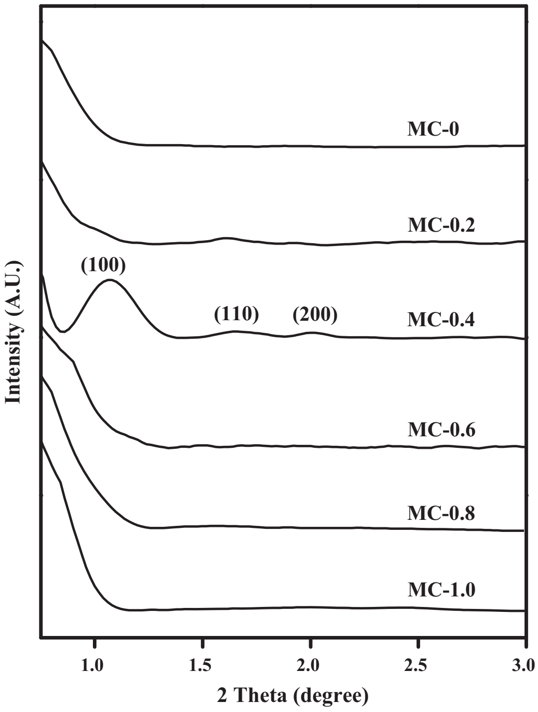

Fig. 4. SAXS patterns of MC-*X* supports.

HR-TEM images of MC-0.4 support are shown in Fig. 5. It was clearly observed that MC-0.4 was composed of 2-D hexagonally ordered nanorod array (diameter of the carbon rod is ca. 6 nm). These HR-TEM images strongly indicate that MC-0.4 support retains regular structure and mesoporosity.

3.2. Physical properties of Re/MC-X catalysts

Physical properties of Re/MC-*X* catalysts (*X* = 0, 0.2, 0.4, 0.6, 0.8, and 1.0) are summarized in Table 1. Re/MC-0.4 support showed the highest surface area (1124 m^2/g) and largest pore volume (1.62 cm^3/g). Surface area and pore volume increased with increasing H_2SO_4 concentration in the Re/MC-*X* (*X* = 0, 0.2, and 0.4) catalysts. On the other hand, surface area and pore volume decreased with increasing H_2SO_4 concentration in the Re/MC-*X* (*X* = 0.4, 0.6, 0.8, and 1.0) catalysts. Moreover, micropore was developed at high H_2SO_4 concentration. This means that H_2SO_4 treatment at high concentration may cause destruction of pore channel, leading to the increase of microporosity and the decrease of mesoporosity. As listed in Table 1, surface area and pore volume of the catalysts showed volcano-shaped trends with respect to H_2SO_4 concentration.

Table 1
Physical properties of Re/MC-*X* catalysts.

	Surface area (m^2/g-cat.)	Micropore area (m^2/g-cat.)	Pore volume (cm^3/g-cat.)
Re/MC-0	868	–	1.25
Re/MC-0.2	911	–	1.30
Re/MC-0.4	1124	–	1.62
Re/MC-0.6	906	107	1.31
Re/MC-0.8	596	284	0.68
Re/MC-1.0	448	274	0.42

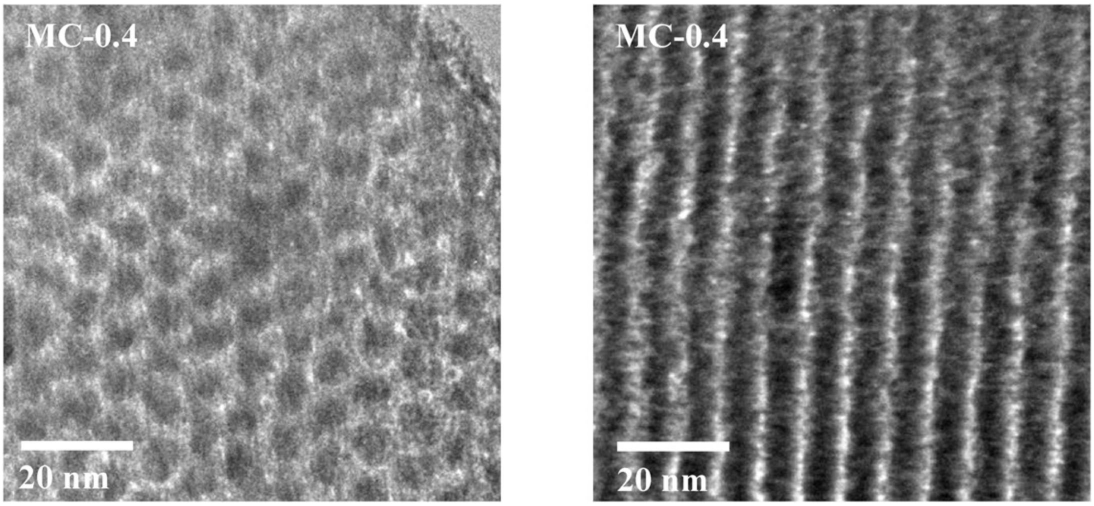

Fig. 5. HR-TEM images of MC-0.4 support.

Fig. 6 shows the nitrogen adsorption–desorption isotherms of Re/MC-X (X = 0, 0.4, and 0.8) catalysts. All the Re/MC-X catalysts showed type-IV isotherms. Both Re/MC-0 and Re/MC-0.4 catalysts showed type-H3 hysteresis loop, indicating the existence of mesoporosity [25]. In particular, Re/MC-0.4 showed more apparent type-H3 hysteresis loop than Re/MC-0 catalyst. This implies that mesoporosity of Re/MC-0.4 was developed by H_2SO_4 treatment. On the other hand, Re/MC-0.8 catalyst showed type-H4 hysteresis loop, indicating the increase of microporosity. These physical properties of Re/MC-X catalysts were well consistent with FE-SEM and SAXS results of MC-X supports (Figs. 3 and 4). The above results indicate that pore structure of MC-X supports could be controlled by changing H_2SO_4 treatment concentration.

3.3. Rhenium particle size and metal–support interaction of Re/MC-X catalysts

Fig. 7 shows the HR-TEM images of Re/MC-X catalysts (X = 0, 0.2, 0.4, 0.6, 0.8, and 1.0) reduced at 450 °C. In the Re/MC-X catalysts (X = 0, 0.2, and 0.4), rhenium particle size became smaller with increasing H_2SO_4 concentration. In the Re/MC-X catalysts (X = 0.6, 0.8, and 1.0), however, rhenium particle size became larger with increasing H_2SO_4 concentration. These were well consistent with the trends of surface area and pore volume of MC-X supports (Table 1) with regard to H_2SO_4 concentration. It is known that large pore volume and ordered mesoporosity are mainly responsible for enhancing dispersion of metal particle in the supported metal catalyst. Therefore, Re/MC-0.4 catalyst with the largest pore volume and most regular mesoporous structure showed the smallest rhenium particle size (less than 5 nm) among the Re/MC-X catalysts.

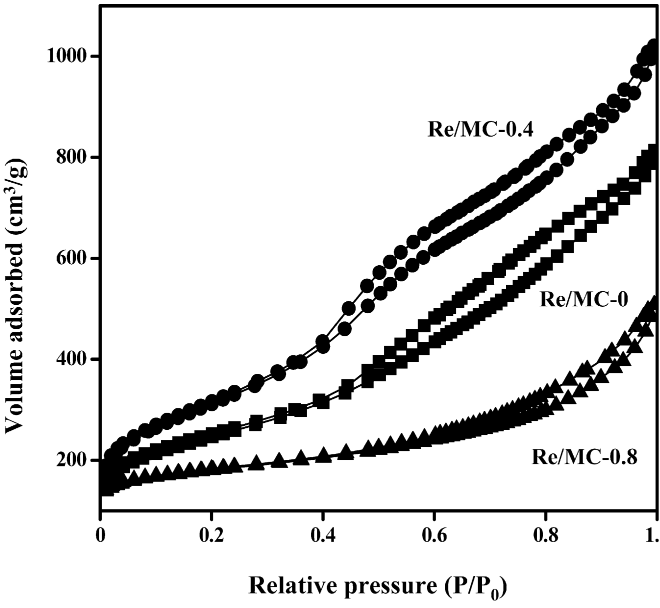

Fig. 6. Nitrogen adsorption–desorption isotherms of Re/MC-X catalysts reduced at 450 °C.

In order to ensure the trend of rhenium dispersion (rhenium particle size) of Re/MC-X catalysts, TPR measurements were conducted. TPR results of Re/MC-X catalysts are shown in Fig. 8. With increasing H_2SO_4 concentration, reduction peak temperature of Re/MC-X catalysts (X = 0, 0.2, and 0.4) decreased, while that of Re/MC-X (X = 0.6, 0.8, and 1.0) catalysts increased. In other words, metal–support interaction of Re/MC-X catalysts (X = 0, 0.2, and 0.4) decreased while that of Re/MC-X (X = 0.6, 0.8, and 1.0) increased with increasing H_2SO_4 concentration. Interestingly, the trend of TPR peak temperature was well consistent with the trend of surface area and pore volume of MC-X supports (Table 1).

Table 2 shows the hydrogen uptake and rhenium particle size of Re/MC-X (X = 0, 0.2, 0.4, 0.6, 0.8, and 1.0) catalysts. Rhenium particle size and hydrogen uptake were calculated on the basis of TPR peak area using the equations in literatures [26,27]. Rhenium particle size of Re/MC catalysts showed the same trend as TPR peak temperature with respect to H_2SO_4 concentration. This means that rhenium particle is finely dispersed on the MC support when the metal–support interaction is weak. It is believed that small metal particle has a weak interaction with the support due to small interfacial area between two solids by geometric effect [28,29]. In other words, when the interaction between metal and support is stronger, metal particle can spread out over the support,

Table 2
Hydrogen uptake and rhenium particle size of Re/MC-X catalysts.

	Hydrogen uptake (mmol/g-cat.)	Rhenium particle size (nm)
Re/MC-0	1.57	9.1
Re/MC-0.2	3.27	4.4
Re/MC-0.4	3.66	3.9
Re/MC-0.6	2.44	5.8
Re/MC-0.8	1.07	13.3
Re/MC-1.0	0.51	27.8

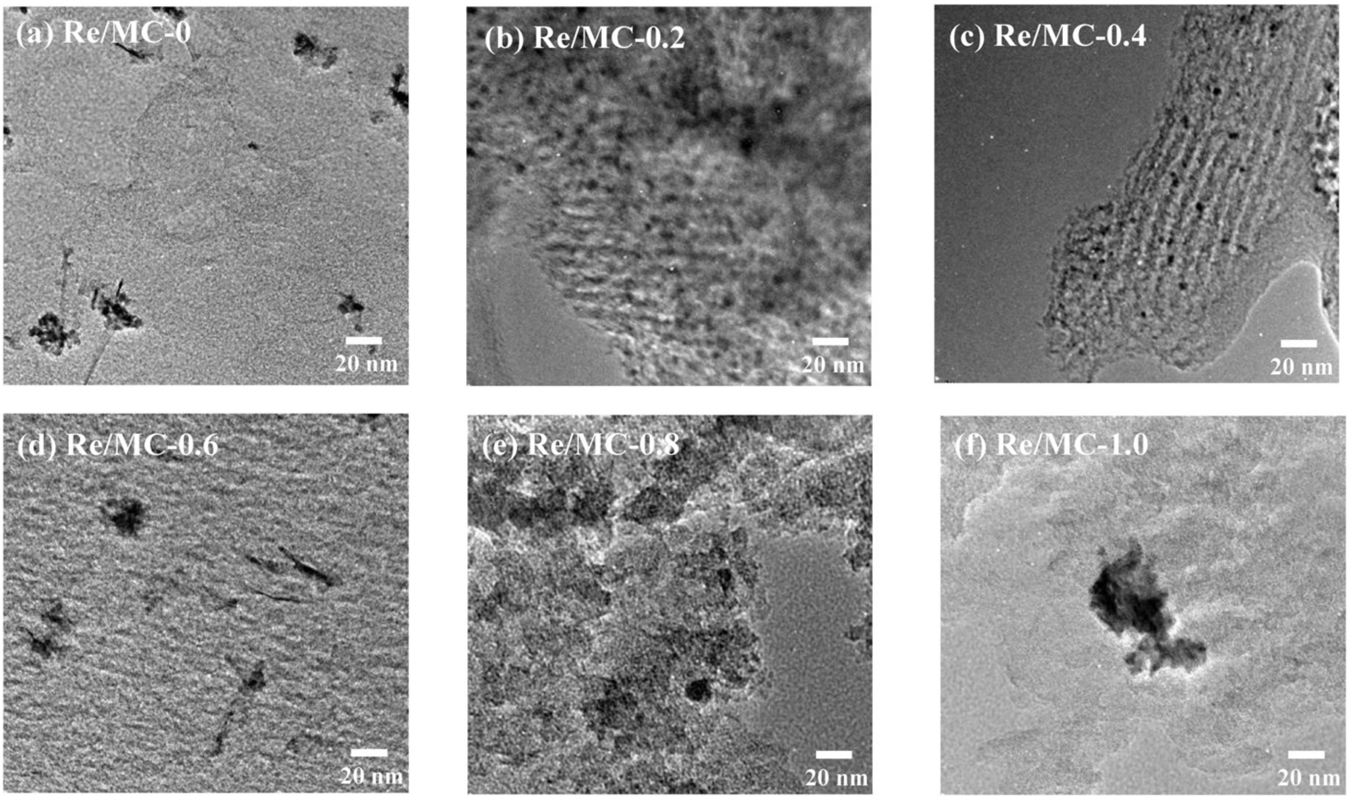

Fig. 7. HR-TEM images of Re/MC-*X* catalysts reduced at 450 °C.

so that the metal particle size becomes larger. For this reason, Re/MC-*X* catalyst with smaller rhenium particle size and higher hydrogen uptake capacity showed lower reduction temperature in TPR profile. Among the Re/MC-*X* catalysts, Re/MC-0.4 catalyst showed the smallest rhenium particles (3.9 nm) and the highest hydrogen uptake capacity (3.66 mmol/g-cat.), while Re/MC-1.0 catalyst showed the largest rhenium particle size (27.8 nm) and the smallest hydrogen uptake capacity (0.51 mmol/g-cat.). Once again, it is noticeable that rhenium particle size (Table 2), TPR peak temperature (Fig. 8), and surface area and pore volume of supports (Table 1) showed the same trends with respect to H_2SO_4 treatment concentration.

3.4. Hydrogenation of succinic acid (SA) over Re/MC-X catalysts

Catalytic performance of Re/MC-*X* catalysts (X = 0, 0.2, 0.4, 0.6, 0.8, and 1.0) in the liquid-phase hydrogenation of succinic acid (SA) is shown in Table 3. γ-Butyrolactone (GBL), tetrahydrofuran (THF), and 1,4-butanediol (BDO) were produced as main products via hydrogenation of succinic acid. Ethanol was mainly produced as a by-product via hydrogenolysis and oxidative-hydrogenation of succinic acid, and small amounts of acetic acid and butyric acid were also produced as by-products. It is known that rhenium is an effective catalyst for hydrogenolysis and oxidative-hydrogenation [14,30,31]. Therefore, the side reaction (formation of ethanol) competitively occurred together with hydrogenation of succinic acid (formation of THF) over the supported rhenium catalyst.

Table 3
Catalytic performance of Re/MC-*X* catalysts in the liquid-phase hydrogenation of succinic acid (reaction temperature = 240 °C; reaction pressure = 80 bar; reaction time = 8 h).

	Conversion of SA (%)	Yield (%)			
		GBL	THF	BDO	By-products
Re/MC-0	80.4	62.2	7.3	3.1	7.8
Re/MC-0.2	99.4	48.6	26.4	3.1	21.3
Re/MC-0.4	100	26.8	38.3	4.5	30.4
Re/MC-0.6	85	61.1	8.9	3.4	11.6
Re/MC-0.8	61.8	44.9	5.1	3.1	8.7
Re/MC-1.0	51.3	38.1	3.6	2.4	7.2

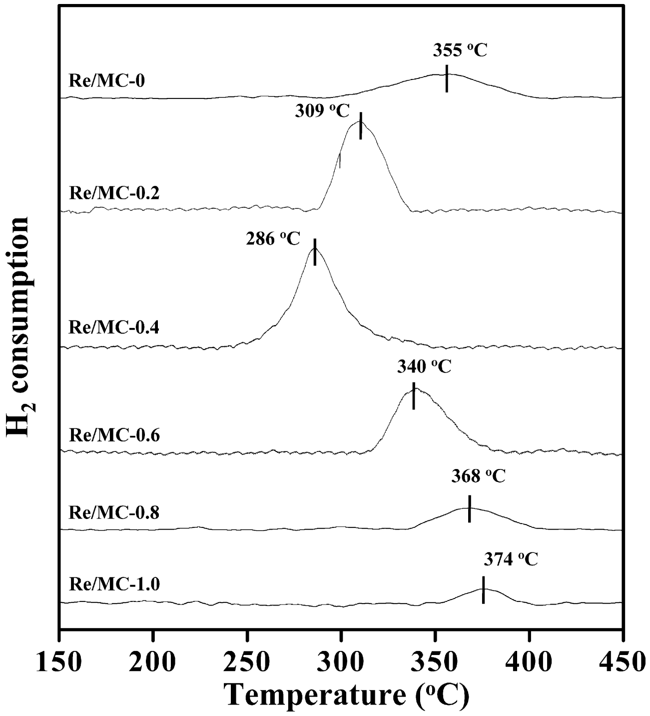

Fig. 8. TPR profiles of Re/MC-*X* catalysts.

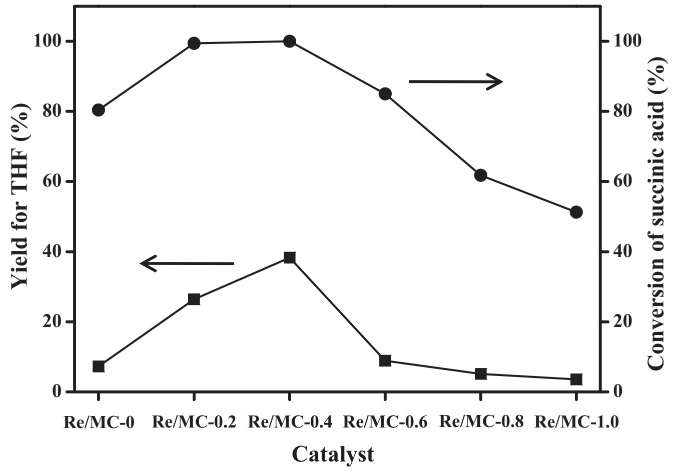

Fig. 9. Catalytic activity of Re/MC-*X* catalysts in the liquid-phase hydrogenation of succinic acid to THF (reaction temperature = 240 °C; reaction pressure = 80 bar; reaction time = 8 h).

Fig. 9 shows the catalytic performance of Re/MC-*X* catalysts in the liquid-phase hydrogenation of succinic acid. It is noteworthy that both conversion of succinic acid and yield for THF showed volcano-shaped curves with respect to H_2SO_4 concentration. This means that an optimal H_2SO_4 concentration was required for maximum catalytic performance. Among the catalyst tested, Re/MC-0.4 catalyst showed the highest conversion of succinic acid (100%) and the highest yield for THF (38.3%), while Re/MC-1.0 catalyst showed the lowest conversion of succinic acid (51.3%) and the lowest yield for THF (3.6%). It is believed that the excellent catalytic performance of Re/MC-0.4 catalyst was due to the smallest rhenium particle size (the highest rhenium dispersion).

In order to investigate the effect of rhenium particle size of Re/MC-*X* catalysts on the catalytic activity in the hydrogenation of succinic acid, a correlation between rhenium particle size of Re/MC-*X* catalysts and yield for THF was established. Fig. 10 shows the correlation between rhenium particle size of Re/MC-*X* catalysts and yield for THF in the hydrogenation of succinic acid. It was observed that yield for THF increased with decreasing rhenium particle size (with increasing rhenium dispersion) of Re/MC-*X* catalysts. This result strongly supports that rhenium particle size of Re/MC-*X* catalysts served as an important factor determining the catalytic performance in the hydrogenation of succinic acid to THF.

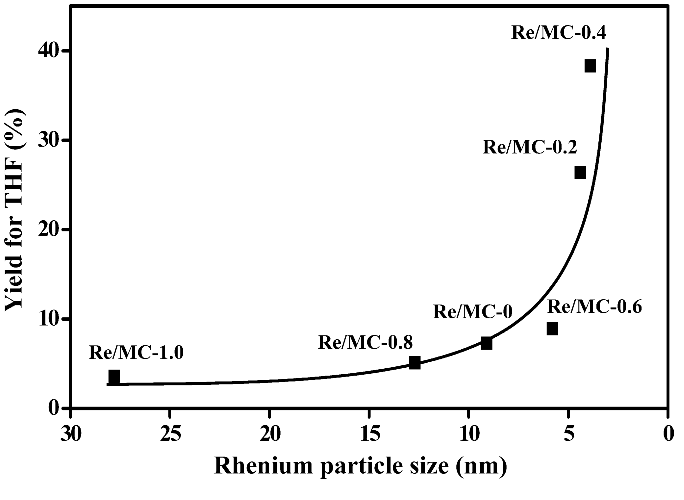

Fig. 10. A correlation between rhenium particle size of Re/MC-*X* catalysts and catalytic activity in the hydrogenation of succinic acid to THF.

Table 4
Result for liquid-phase hydrogenation of succinic acid over Re/MC-0.4 catalyst with respect to recycle run (reaction temperature = 240 °C; reaction pressure = 80 bar; reaction time = 8 h).

Recycle run	Conversion of SA (%)	Yield for THF (%)	Rhenium leaching[a] (ppm)
1	100	38.1	0.84
2	100	37.4	0.77
3	100	37.2	0.61

[a] Determined by ICP-AES analyses.

3.5. *Stability and reusability of Re/MC-X catalyst*

To investigate the stability and reusability of the catalyst, recycle tests for hydrogenation of succinic acid over Re/MC-0.4 catalyst were performed three times. Table 4 shows the result for liquid-phase hydrogenation of succinic acid to THF over Re/MC-0.4 catalyst with respect to recycle run. It was found that fresh and spent catalysts showed similar catalytic activity. Furthermore, no significant rhenium leaching (less than 1.0 ppm) was detected by ICP-AES analysis after each reaction test. Thus, Re/MC-0.4 catalyst served as a stable and reusable catalyst in the hydrogenation of succinic acid to THF.

3.6. *Comparison of catalytic performance of supported rhenium catalysts (Re/CA-0.4, Re/PC-0.4, and Re/MC-0.4)*

Catalytic performance of Re/CA-0.4, Re/PC-0.4, and Re/MC-0.4 in the liquid-phase hydrogenation of succinic acid to THF is shown in Fig. 11. In the hydrogenation of succinic acid over Re/CA-0.4 and Re/PC-0.4 catalysts, γ-butyrolactone (GBL), tetrahydrofuran (THF), and 1,4-butanediol (BDO) were also produced as main products via hydrogenation of succinic acid. In the comparison test, Re/MC-0.4 catalyst showed the highest conversion of succinic acid (100%) and the highest yield for THF (38.3%). Re/CA-0.4 and Re/PC-0.4 catalysts showed lower conversion of succinic acid (60.9% and 72.3%, respectively) and lower yield for THF (4.1% and 5.2%, respectively) than Re/MC-0.4 catalyst. It is believed that the excellent catalytic performance of Re/MC-0.4 catalyst was due to the smallest rhenium particle size. Rhenium particle size of Re/MC-0.4 catalyst was 3.9 nm (Table 2), while that of Re/CA-0.4 and Re/PC-0.4 catalysts was 15.5 nm and 9.7 nm, respectively. This result also supports that rhenium particle size of the supported catalysts served as a key factor determining the catalytic performance in the hydrogenation of succinic acid to THF.

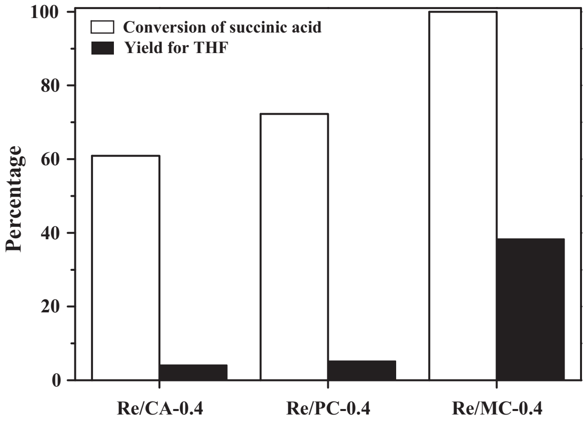

Fig. 11. Comparison of catalytic performance of Re/CA-0.4, Re/PC-0.4, and Re/MC-0.4 in the hydrogenation of succinic acid to THF (reaction temperature = 240 °C; reaction pressure = 80 bar; reaction time = 8 h).

4. Conclusions

Mesoporous carbon (MC) prepared by a surfactant-templating method was treated with different H_2SO_4 concentration ($X = 0$, 0.2, 0.4, 0.6, 0.8, and 1.0 M). Rhenium catalysts supported on H_2SO_4-treated mesoporous carbons (Re/MC-*X*) were then prepared by an incipient wetness impregnation method. Among the Re/MC-*X* ($X = 0$, 0.2, 0.4, 0.6, 0.8, and 1.0) catalysts, Re/MC-0.4 catalyst showed the smallest rhenium particle size due to the regularly developed mesoporous structure of MC-0.4. In the hydrogenation of succinic acid, both conversion of succinic acid and yield for THF showed volcano-shaped curves with respect to H_2SO_4 concentration. Thus, an optimal H_2SO_4 concentration for the treatment of MC was required to achieve maximum yield for THF. Yield for THF in the hydrogenation of succinic acid increased with decreasing rhenium particle size of Re/MC-*X* catalysts. Thus, rhenium particle size played a key role in determining the catalytic performance in the hydrogenation of succinic acid to THF over Re/MC-*X* catalysts. In the recycle test, Re/MC-0.4 catalyst served as a stable and reusable catalyst for hydrogenation of succinic acid to THF. Furthermore, Re/MC-0.4 catalyst showed a better catalytic performance than Re/CA-0.4 and Re/PC-0.4 catalysts in the hydrogenation of succinic acid to THF.

Acknowledgment

This subject is supported by Korea Ministry of Environment as “Converging Technology Project (202-091-001)”.

References

[1] J. Keneta, T. Asano, S. Masamune, Ind. Eng. Chem. 62 (1970) 24–32.
[2] V. Pallassana, M. Neurok, G. Coulston, Catal. Today 50 (1999) 589–601.
[3] S.P. Müller, M. Kucher, C. Ohlinger, B. Kraushaar-Czarnetzkyi, J. Catal. 218 (2003) 419–426.
[4] S.M. Jung, E. Godard, S.Y. Jung, K.-C. Park, J.U. Choi, J. Mol. Catal. A 198 (2003) 297–302.
[5] S.E. Hunter, C.E. Ehrenberger, P.E. Savage, J. Org. Chem. 71 (2006) 6229–6239.
[6] M.D. Wildberger, M. Maciejewski, J.-D. Grunwaldt, T. Mallat, A. Baiker, Appl. Catal. A 179 (1999) 189–202.
[7] U.G. Hong, S. Hwang, J.G. Seo, J. Yi, I.K. Song, Catal. Lett. 138 (2010) 28–33.
[8] C. Delhomme, D. Weuster-Botz, F.E. Kühn, Green Chem. 11 (2009) 13–26.
[9] A. Cukalovic, C.V. Stevens, Biofuels Bioprod. Bioref. 2 (2008) 505–529.
[10] I. Bechthold, K. Bretz, S. Kabasci, R. Kopitzky, A. Springer, Chem. Eng. Technol. 31 (2008) 647–654.
[11] C. Du, S.K.C. Lin, A. Koutinas, R. Wang, C. Webb, Appl. Microbiol. Biotechnol. 76 (2007) 1263–1270.
[12] L. Rosi, M. Frediani, P. Frediani, J. Org. Chem. 695 (2010) 1314–1322.
[13] R. Luque, J.H. Clark, K. Yoshida, P.L. Gai, Chem. Commun. (2009) 5303–5307.
[14] D.P. Mihn, M. Besson, C. Pinel, P. Fuertes, C. Petitjean, Top. Catal. 53 (2010) 1270–1273.
[15] J.G. Seo, M.H. Youn, K.M. Cho, S. Park, S.H. Lee, J. Lee, I.K. Song, Korean J. Chem. Eng. 25 (2008) 41–45.
[16] P. Kim, J.B. Joo, W. Kim, J. Kim, I.K. Song, J. Yi, Catal. Lett. 112 (2006) 213–218.
[17] H. Kim, J.C. Jung, D.R. Park, S.-H. Baeck, I.K. Song, Appl. Catal. A 320 (2007) 159–165.
[18] U.G. Hong, D.R. Park, S. Park, J.G. Seo, Y. Bang, S. Hwang, M.H. Youn, I.K. Song, Catal. Lett. 132 (2009) 377–382.
[19] J. Kim, J. Lee, T. Hyeon, Carbon 42 (2004) 2711–2719.
[20] L. Li, H. Song, X. Chen, Micropor. Mesopor. Mater. 94 (2006) 9–14.
[21] Y.J. Lee, J.C. Jung, J. Yi, S.-H. Baeck, J.R. Yoon, I.K. Song, Curr. Appl. Phys. 10 (2010) 682–686.
[22] H.W. Park, U.G. Hong, Y.J. Lee, I.K. Song, Appl. Catal. A 409–410 (2011) 167–173.
[23] D.W. Wang, F. Li, H.T. Fang, M. Liu, G.Q. Lu, H.M. Cheng, J. Phys. Chem. B 110 (2006) 8570–8575.
[24] H. Kim, P. Kim, K.-Y. Lee, S.H. Yeom, J. Yi, I.K. Song, Catal. Today 111 (2006) 361–365.
[25] K.S.W. Sing, D.H. Everett, R.A.W. Haul, L. Moscou, R.A. Pierotti, J. Rouquérol, T. Siemieniewska, Pure Appl. Chem. 57 (1985) 602–619.
[26] J.J.F. Scholten, A.P. Pijpers, A.M.L. Hustings, Catal. Rev. 27 (1985) 151–206.
[27] A. Borodziński, M. Bonarowska, Langmuir 13 (1997) 5613–5620.
[28] E. Antolini, Appl. Catal. B 88 (2009) 1–24.
[29] R.L. Augustine, Heterogeneous Catalysis for the Synthetic Chemists, Marcel Dekker, New York, 1996.
[30] J.F. Le Page, Applied Heterogeneous Catalysis: Design, Manufacture, Use of Solid Catalysts, Editions Technip, Paris, 1987.
[31] H.S. Broadbent, Ann. N.Y. Acad. Sci. 145 (1967) 58–71.